The Journal of Experimental Biology 206, 4125-4137

doi:10.1242/jeb.00649

The ontogenetic scaling of hydrodynamics and swimming performance in jellyfish (*Aurelia aurita*)

Matthew J. McHenry[1,*] and Jason Jed[2]

[1]*The Museum of Comparative Zoology, Harvard University, 26 Oxford St, Cambridge, MA 02138, USA* and
[2]*The Department of Integrative Biology, University of California, Berkeley, CA 94720, USA*

*Author for correspondence (e-mail: mchenry@fas.harvard.edu)

Accepted 6 August 2003

Summary

It is not well understood how ontogenetic changes in the motion and morphology of aquatic animals influence the performance of swimming. The goals of the present study were to understand how changes in size, shape and behavior affect the hydrodynamics of jet propulsion in the jellyfish *Aurelia aurita* and to explore how such changes affect the ontogenetic scaling of swimming speed and cost of transport. We measured the kinematics of jellyfish swimming from video recordings and simulated the hydrodynamics of swimming with two computational models that calculated thrust generation by paddle and jet mechanisms. Our results suggest that thrust is generated primarily by jetting and that there is negligible thrust generation by paddling. We examined how fluid forces scaled with body mass using the jet model. Despite an ontogenetic increase in the range of motion by the bell diameter and a decrease in the height-to-diameter ratio, we found that thrust and acceleration reaction scaled with body mass as predicted by kinematic similarity. However, jellyfish decreased their pulse frequency with growth, and speed consequently scaled at a lower exponential rate than predicted by kinematic similarity. Model simulations suggest that the allometric growth in *Aurelia* results in swimming that is slower, but more energetically economical, than isometric growth with a prolate bell shape. The decrease in pulse frequency over ontogeny allows large *Aurelia* medusae to avoid a high cost of transport but generates slower swimming than if they maintained a high pulse frequency. Our findings suggest that ontogenetic change in the height-to-diameter ratio and pulse frequency of *Aurelia* results in swimming that is relatively moderate in speed but is energetically economical.

Key words: swimming, morphology, scaling, jetting, scyphomedusae, locomotion, jellyfish, *Aurelia aurita.*

Introduction

The performance of swimming may change dramatically over the growth of an aquatic animal. Despite our understanding of the broad-scale hydrodynamic differences in the swimming of animals spanning many orders of magnitude in body length (Daniel et al., 1992; Lighthill, 1975; Wu, 1977), we cannot predict how ontogenetic changes in the size, shape and motion of the body influence the speed and energetic cost of swimming within individual species. The purpose of the present study was to examine the scaling of hydrodynamic forces in the jellyfish *Aurelia aurita* in order to understand how such ontogenetic changes affect swimming performance.

The ontogenetic scaling of swimming performance

Although it is generally appreciated that a fully grown aquatic animal will swim faster than when it was smaller, the precise relationship between speed and body size over a life history is dictated by scale-dependent hydrodynamics. Much of our understanding for this scale dependency comes from comparisons between species that differ in body mass by many orders of magnitude (e.g. Daniel et al., 1992; Lighthill, 1975; Wu, 1977). These comparisons illustrate that thrust is generated primarily by viscous force at the size of spermatozoa, inertial force at the size of adult fish and a combination of these forces at intermediate sizes. Such broad comparisons are useful for understanding the major fluid forces that play a role in the hydrodynamics of a growing animal but cannot provide predictive explanations for how swimming performance (e.g. speed and cost of transport) should change over the ontogeny of individual species.

Ontogenetic changes in swimming kinematics have been most thoroughly explored in larval fish (e.g. Batty, 1984; Fuiman, 1993; Fuiman and Webb, 1988; Hale, 1999; Hunter, 1972; Hunter and Kimbrell, 1980; Osse and van den Boogaart, 2000), which propel themselves by lateral tail undulation. During routine swimming, larval fish generally beat their tails with greater length-specific amplitude but propel themselves at lower speed than adults of the same species. Although it is appreciated that force generated by the inertia of water increases in importance relative to viscous force as fish grow larger (Fuiman and Batty, 1997; McHenry et al., 2003; Muller

et al., 2000; Webb and Weihs, 1986), few investigators have tested whether a hydrodynamic model is capable of predicting the scaling of swimming performance in fish (although Vlymen, 1974 is an exception). Such an approach would allow an investigator to explore the relative contribution of inertial and viscous forces to thrust and drag and to evaluate whether alternative larval morphology or tail kinematics could improve on swimming performance.

Although the scaling of swimming performance is not as well characterized for aquatic invertebrates as for larval fish, some investigators have used a combination of modeling and experimentation in order to understand the hydrodynamic mechanisms that explain the scaling of performance in invertebrate species. Using such an approach, Williams (1994) demonstrated that the serial addition of developing limbs along the abdomen of the brine shrimp (*Artemia* sp.) initially does not contribute to propulsion when larvae are small, but the additional limbs generate thrust in later life history stages when unsteady forces play a greater role in the hydrodynamics of swimming. Using a combination of kinematics and force measurements, Nauen and Shadwick (2001) found that the tail of the spiny lobster (*Panulirus interruptus*) generates most of its force with a paddle mechanism and that maximum force production scales according to a paddle model. Dadswell and Weihs (1990) determined that giant scallops (*Placopecten magellanicus*) swim with the greatest speed at a medium body size range, when they attain the highest thrust-to-weight ratio of their life history.

Jellyfish are a potentially useful group for exploring the ontogenetic scaling of hydrodynamics because their swimming is easily modeled. Daniel (1983) proposed a mathematical model that suggested that the hydrodynamics of prolate (bullet-shaped) hydromedusae are dominated by the thrust generated by jetting, the acceleration reaction (i.e. the force generated by accelerating the water around the body) and the drag resisting the forward motion of the body. This model replicated observed oscillations in swimming speed (Daniel, 1983), and Colin and Costello (2002) found the model to accurately predict body acceleration in prolate, but not oblate (plate-shaped), jellyfish. They proposed that oblate jellyfish generate thrust primarily by paddling the flexible margins of their bell instead of using a jet mechanism. We tested this hypothesis by comparing measurements of speed in *Aurelia*, an oblate jellyfish, with predictions from mathematical models of swimming that assume thrust generation by either paddling or jetting.

Geometric and kinematic similarity

Changes in the shape or relative motion of an animal's body during growth should be reflected in the allometric scaling of morphometric and kinematic parameters (Huxley, 1932; McMahon, 1984). An allometric relationship is defined as a deviation from isometry (Schmidt-Nielsen, 1984) and therefore requires the formulation of an *a priori* null hypothesis as predicted by isometry. In complex biomechanical systems, these predictions are not always obvious and therefore merit careful consideration (e.g. Hernandez, 2000; Nauen and Shadwick, 2001; Quillin, 2000; Rome, 1992).

If a jellyfish grows isometrically, then its bell height, h, scales linearly with bell diameter, d, and medusae at all sizes will be geometrically similar (i.e. $h \propto d$). Geometric similarity implies that the volume of the body scales as d^3, which means that bell diameter scales with body mass (m) as $m^{1/3}$ (assuming constant tissue density). During swimming, the shape of the bell changes with time. Bell height rapidly increases and bell diameter rapidly decreases over a pulse phase (Gladfelter, 1973). To achieve kinematic similarity (Quillin, 1999), a jellyfish must maintain the speed of height change in proportion to the speed of diameter change at all body sizes. In geometrically similar jellyfish, kinematic similarity is maintained if the pulse frequency, duty factor (the proportion of the propulsive cycle spent pulsing) and range of motion remain constant. Kinematic similarity also requires that a jellyfish moves through the water at a speed that is directly proportional to d and therefore scales as $m^{1/3}$. This form of kinematic similarity has been observed in fish made to swim steadily at the same frequency (Bainbridge, 1958).

Geometric and kinematic similarity suggest predictions for the scaling of hydrodynamic forces in jetting jellyfish. Drag scales with the area of the bell ($\propto d^2$) and the square of swimming speed ($\propto d^2$; Daniel, 1983), which suggests that this force scales as d^4 and $m^{4/3}$. Thrust scales with the inverse of the area of the subumbrellar opening through which water jets ($\propto d^{-2}$) and the square of the rate of change in bell volume ($\propto d^6$), suggesting that thrust also scales as d^4 and $m^{4/3}$. The acceleration reaction varies with the volume of the body ($\propto d^3$) and its rate of change in velocity ($\propto d$, assuming sinusoidal changes in velocity), which implies that this force also scales as d^4 and $m^{4/3}$. Since all three hydrodynamic forces are predicted to scale with mass in the same way, we predict that the hydrodynamics of swimming should not change if jellyfish maintain geometric and kinematic similarity. Conversely, scaling that deviates from this null hypothesis implies that the hydrodynamics of jetting changes with size. These scaling predictions assume that the jellyfish operate at relatively high, inertia-dominated, Reynolds numbers.

The present study

We pursued three objectives in order to address how ontogenetic changes affect the swimming performance of *Aurelia*. (1) The hydrodynamics of swimming were modeled with paddle and jet mechanisms in separate simulations in order to test which mechanism more accurately predicts swimming speed. (2) The scaling of relationships of parameters that play a role in the dynamics of swimming were measured. (3) The performance of swimming in *Aurelia* was compared with that predicted for model jellyfish exhibiting different patterns of growth.

Aurelia is a marine scyphozoan with an oblate medusa stage that spans over an order of magnitude in bell diameter (Meinkoth, 1995). This large change in body size makes *Aurelia* an ideal system for examining the scaling of

swimming performance. The swimming of medusae such as *Aurelia* is thought to affect their position in the water column and thereby influence dispersal and movement into areas of high prey density and favorable environmental conditions within the plankton (Buecher and Gibbons, 1999; Johnson et al., 2001; Mutlu, 2001; Nicholas and Frid, 1999). The bell pulsing used by *Aurelia* to swim also facilitates mass transport and prey capture by increasing with flow over the bell and tentacles (Costello and Colin, 1994; Daniel, 1983; Mills, 1981).

Materials and methods

Kinematics and morphometrics

We measured the shape and swimming movement of medusae of *Aurelia aurita* (L.) from video recordings made at the Monterey Bay Aquarium, Pacific Grove, CA, USA. Medusae ranging in bell diameter from 1.57 cm to 9.51 cm were held in aquaria containing natural seawater at 16°C. These tanks were sufficiently large (15 cm deep × 17 cm × 15 cm wide for bell diameters less than 4 cm, and 61 cm deep × 65 cm × 28 cm wide for bell diameters greater than 4 cm) to avoid wall effects when individual animals were video recorded (30 frames s^{-1}; Panasonic PV-S62D SVHS-C Camcorder) in the tank's center (Vogel, 1981). The mean tissue density, ρ_{tissue}, of each jellyfish was calculated as the ratio of measured body mass and the body volume, which was found by water displacement in a graduated cylinder.

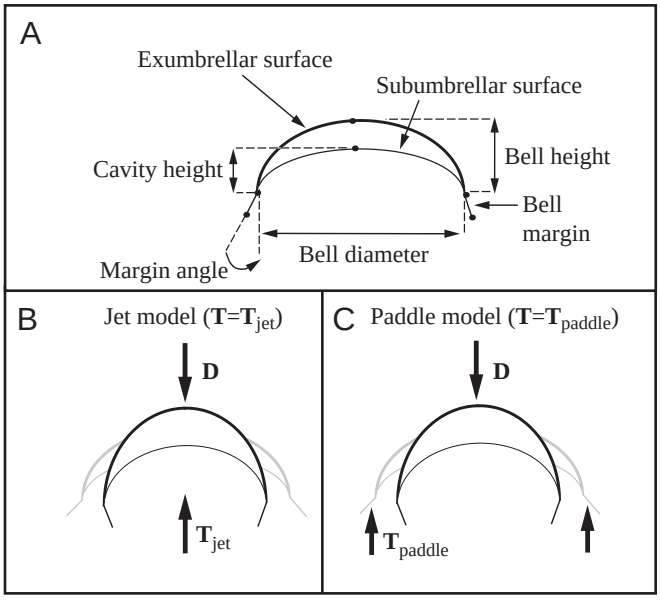

Fig. 1. Morphometrics and hydrodynamic modeling. (A) The filled dots show the landmarks used to reconstruct the shape of the body and provide measurements for the parameters noted. (B,C) The two hydrodynamic models used in the present study are illustrated with the drag, **D**, and thrust, **T**, vectors predicted to be generated as the bell contracts and the bell margin adducts. (B) The jet model assumes thrust to be generated by a jet, $\mathbf{T}_{jet}$. (C) The paddle model assumes thrust is generated by paddling, $\mathbf{T}_{paddle}$.

The motion of jellyfish was measured by following the movement of landmarks on the bell using NIH Image on an Apple Macintosh G3 computer (Fig. 1A). We tracked the movement of the exumbrellar and subumbrellar surfaces along the central axis and defined the bell margin as the ring of flexible tissue running from the distal margin of the bell (where the tentacles begin) to a proximal line of high bending. From these data, we calculated the bell height, h, as the distance between the exumbrellar surface and the opening of the subumbrellar cavity along the central axis; the cavity height, h_{cav}, as the distance between the subumbrellar surface and the opening of the subumbrellar cavity; the diameter of the bell, d, as the distance between lateral surfaces of the bell; and the margin angle, θ, as the angle between the central axis and the margin of the bell (Fig. 1A). We described the passive shape of the bell by measuring the diameter, d_{rest}, and height, h_{rest}, of each animal while at rest from video images. The height-to-diameter ratio for each individual was calculated as the quotient of these quantities. The pulse frequency, f, and the duty factor, q, which is the ratio of the period of the pulse phase and the period of the whole propulsive cycle, were measured over a duration of three to five propulsive cycles. The range of values in margin angle, θ_{range}, cavity height, h_{range}, and bell diameter, d_{range}, were also recorded.

We described the scaling of individual kinematic and morphological parameters, y, with body mass, m, using the scaling constant, a, and scaling exponent, b, of an exponential function ($y=am^b$). These values were found from the intercept and slope of a reduced major axis regression fit to log-transformed data. We rejected the null hypothesis, b_o, in cases where predictions fell outside of the lower, L_1, and upper, L_2, 95% confidence intervals about the slope of the regression (Rayner, 1985; Sokal and Rohlf, 1995). This form of Type II regression was appropriate because the scale and dimensions of our independent and dependent variables were not equal and the error for each variable was unknown. The coefficient of determination, r^2, was used to assess the degree of variation explained by reduced major axis regressions.

Hydrodynamic forces

As in Daniel (1983), we modeled the hydrodynamics of jellyfish swimming as the sum of thrust, **T**, drag, **D**, the acceleration reaction force, **A**, and the force acting to change the inertia of the body, **F**. This model is expressed in an equation of motion as:

$$\mathbf{T} + \mathbf{D} + \mathbf{A} + \mathbf{F} = 0 \ . \quad (1)$$

Drag was calculated with the following equation (Batchelor, 1967):

$$\mathbf{D} = 0.5 c_{bell} \rho_{water} s_{bell} u \mathbf{U} \ , \quad (2)$$

where s_{bell} is the instantaneous projected area of the bell ($s_{bell}=0.25\pi d^2$, where d varies with time), u and **U** are the instantaneous speed and velocity of the body, respectively, ρ_{water} is the density of seawater, and c_{bell} is the drag coefficient of the bell. We assumed that the drag on the bell was equal to

that of a hemisphere, which has a greater drag coefficient when the body is moving backward (i.e. $\mathbf{U}<0$) than when moving forward (i.e. $\mathbf{U}>0$) (Hoerner, 1965):

$$c_{\text{bell}} = \begin{cases} 0.42 & \text{for } \mathbf{U}>0 \\ 1.17 & \text{for } \mathbf{U}<0 \end{cases} . \quad (3)$$

The acceleration reaction was calculated with the following equation (Daniel, 1983):

$$\mathbf{A} = \alpha\rho_{\text{water}} v(\Delta\mathbf{U}/\Delta t) , \quad (4)$$

where α is the added mass coefficient, v is the volume of the subumbrellar cavity, and t is time. Assuming a hemi-ellipsoid shape to the subumbrellar cavity (as in Daniel, 1985), the instantaneous cavity volume was calculated as follows:

$$v=\pi d^2 h_{\text{cav}}/6 , \quad (5)$$

where the cavity height and diameter of the bell vary with time. The added mass coefficient varies with the shape of the bell (Daniel, 1985):

$$\alpha=(2h/d)^{1.4} . \quad (6)$$

In separate simulations, we modeled the thrust generation by jet and paddle mechanisms (Fig. 1B,C). The thrust generated by jetting, $\mathbf{T}_{\text{jet}}$, was calculated with the following equation (Daniel, 1983):

$$\mathbf{T}_{\text{jet}} = (\rho_{\text{water}}/s_{\text{bell}})(\Delta v/\Delta t)^2 . \quad (7)$$

Negative thrust (i.e. thrust acting to impede forward motion) was generated by this force whenever the cavity volume increased. The thrust generated by paddling, $\mathbf{T}_{\text{paddle}}$, was calculated using the following equation:

$$\mathbf{T}_{\text{paddle}} = \sin(\theta)0.5 c_{\text{margin}}\rho_{\text{water}} s_{\text{margin}} w\mathbf{W} , \quad (8)$$

where c_{margin} is the drag coefficient for the bell margin, w and $\mathbf{W}$ are the speed and velocity, respectively, of the bell margin at the midpoint between its proximal base and distal tip, and s_{margin} is the area of the inside surface of the margin. Since the margin of the bell is a flattened strip of tissue, we modeled it as a flat plate oriented perpendicular to flow (c_{margin}=1.98; Hoerner, 1965). Note that the thrust generated by paddling may also contribute to drag at instances where the velocity of the margin is directed in the aboral direction. We calculated the area of the margin with the following equation for the area of a ring:

$$s_{\text{margin}} = \pi l(d_{\text{rest}} - l) , \quad (9)$$

where l is the length of the bell margin. These hydrodynamic forces acted against the force to change the inertia of the body, which was calculated with the following equation:

$$\mathbf{F} = m(\Delta\mathbf{U}/\Delta t) . \quad (10)$$

Computational modeling

Numerical solutions for swimming speed were calculated using the equation of motion (equation 1) with the measured kinematics of the bell and its margin as input variables. Speed was calculated with a variable order Adams–Bashforth–Moulton solver for integration (Shampine and Gordon, 1975) programmed in MATLAB (version 6.0; Mathworks). Our kinematic equations used a sawtooth function, $k(t)$, which increased linearly over time, t, from values of 0 to 1 over the duration of the pulse phase, then decreased linearly from 1 to 0 over the recovery phase. This function provided an input to the following equations, which we used to describe the motion of the margin angle, bell height and bell diameter:

$$\theta(t) = \theta_{\text{range}} \cos[2\pi k(t) f] , \quad (11)$$

$$h(t) = h_{\text{range}} \sin[2\pi k(t) f] + h_{\text{rest}} , \quad (12)$$

$$d(t) = d_{\text{range}} \{\cos[2\pi k(t) f] - 1\} + d_{\text{rest}} . \quad (13)$$

The mean (time-averaged) speed was calculated from simulations using both the jet model (i.e. $\mathbf{T}=\mathbf{T}_{\text{jet}}$) and the paddle model (i.e. $\mathbf{T}=\mathbf{T}_{\text{paddle}}$) for each jellyfish that we had measure kinematic and morphometric data. Measurements of mean speed were taken over the duration of five propulsive cycles that followed the three cycles that were necessary for the models to reach steady state.

The accuracy of models was tested by comparing the mean swimming speed measured for each jellyfish with the mean speed predicted by simulations run with the same bell and margin kinematics. Experimental sequences were rejected if the mean swimming speed of individual pulses differed by more than 10%. We determined the relationship between measured speed and the speed predicted by simulations with a major axis regression (Rayner, 1985). A model was considered perfectly accurate if the 95% confidence intervals of the slope of this regression, e, included a value of 1. Furthermore, we tested whether models accurately predicted the scaling of speed with body mass by finding the reduced major axis regression for predictions of speed for both models. Models were considered accurate if the 95% confidence intervals of predictions included the measured values for the scaling constant and scaling exponent (Sokal and Rohlf, 1995).

In addition to measuring speed, the hydrodynamic cost of transport, T_{HCOT}, was calculated to assess the performance of each simulation. The hydrodynamic cost of transport is a measure of the total energy invested in jetting to propel a unit mass of the body over a unit distance. It was calculated with the following equation:

$$T_{\text{HCOT}} = \frac{\sum_{i=1}^{n} u_i |\mathbf{T}_i| \Delta t}{mx} , \quad (14)$$

where i is the index for each of the n measurements of speed and the magnitude of thrust, and x is the net distance traversed over the duration of a swimming sequence. This measure of energetic economy neglects internal costs and therefore provides a minimum estimate of metabolic economy.

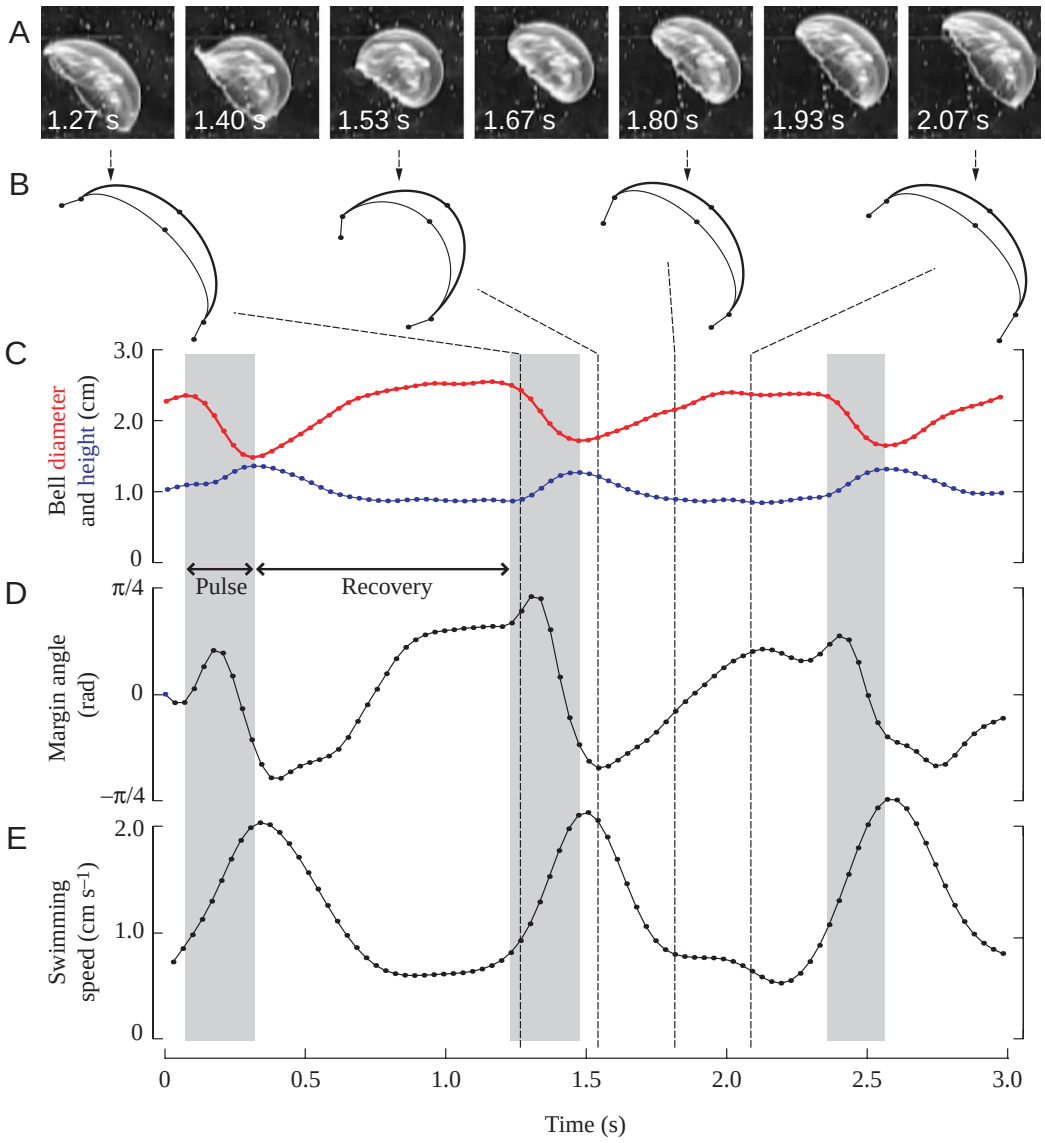

Fig. 2. Representative kinematics of swimming in *Aurelia aurita*. (A) Video frames for one propulsive cycle. (B) The positions of landmarks (filled dots) were used to reconstruct the outer surface of the bell (thick line) and the inner surface of the bell cavity (thin line). (C) Measurements for the bell height (blue line) and diameter (red line) are shown during the pulse (gray band) and recovery (white band) phases of the propulsive cycle. (D) The margin angle and (E) the swimming speed are shown over time.

In order to examine the effects of bell shape and body mass on swimming performance, we ran numerous simulations of our jet model over a range of height-to-diameter ratio and body mass values. Using our data for the scaling of kinematics, we animated the bell with the kinematics appropriate to the body mass used in each simulation. To investigate the effects of ontogenetic changes in behavior on performance, we ran simulations at varying pulse frequency and body mass values. For these simulations, we used the measured values for bell height, bell diameter and pulse frequency specific to body mass. From the results of these simulations, we generated parameter maps describing the effects of body mass, pulse frequency and the height-to-diameter ratio on swimming speed and the hydrodynamic cost of transport. From these parameter maps, we calculated the mean speed and hydrodynamic cost of transport predicted for jellyfish that are geometrically and kinematically similar over the range of measured body mass values.

Results

Jet versus paddle propulsion

During the pulse phase of the propulsive cycle, *Aurelia* medusae rapidly decreased their bell diameter, increased bell height and adducted their bell margin as the body increased in speed (Fig. 2). The body slowed as the bell diameter gradually increased, height decreased and the margin abducted during the recovery phase. Using the kinematics of the bell and margin, thrust predicted by the jet model was generally over an order of magnitude greater than thrust from paddling (Fig. 3). The low thrust generated by paddling resulted in predicted swimming speeds that fell short of measurements (Fig. 4). This was reflected in a major axis regression between measured and predicted speed having a slope with 95% confidence intervals well outside a value of 1 (e=0.002, L_1=–0.015, L_2=0.019, N=19; Fig. 4A). Although the jet model tended to overestimate measured speed (e=1.86, L_1=1.28, L_2=3.02, N=19; Fig. 4B), it provided a more accurate estimate of speed than the paddle

model. The jet model predicted oscillations in speed that closely approximated the variation of speed measured in both large (Fig. 4C) and small (Fig. 4D) jellyfish. Furthermore, the jet model was found to better predict the scaling of swimming speed (see below).

The scaling of morphology, kinematics, hydrodynamics and performance

Our morphometric data suggest that *Aurelia* medusae do not maintain geometric similarity over ontogeny. Jellyfish of high body mass had a bell height that was disproportionately small (b=0.27; Fig. 5A) and a bell diameter that was disproportionately large (b=0.40) compared with jellyfish of low body mass (Fig. 5B; Table 1). This resulted in a significant decrease in the height-to-diameter ratio with increasing body mass (b=–0.16; Fig. 5C). Furthermore, the length of the bell margin scaled by a factor significantly greater than isometry (b=0.43; Table 1).

Aurelia medusae of different body sizes moved with different swimming kinematics. Large jellyfish pulsed at a lower frequency than small jellyfish (b=–0.35), but they maintained similar values for duty factor and the range of margin angle at all sizes (Fig. 6; Table 1). The range of bell diameter scaled by a greater factor (b=0.42) than predicted by kinematic similarity, but the range of bell height did not (b_o=0.33; Table 1). Despite the changes in pulse frequency and the range of bell diameter with body mass, acceleration reaction and thrust scaled with body mass as predicted by kinematic similarity (b_o=1.33; Table 1; Fig. 7A,B). By contrast, drag scaled by a factor (b=0.87) significantly lower than predicted by kinematic similarity (Table 1; Fig. 7C).

Despite pulsing at a lower frequency, larger jellyfish moved with a faster swimming speed than did smaller jellyfish (Fig. 8A). However, the increase in speed with body mass was significantly lower (b=0.17) than predicted by kinematic similarity (Table 1). The jet model consistently overestimated the speed of swimming, which was reflected in its scaling constant (a=–1.4) being significantly greater than the measured value. However, the scaling factor predicted for speed by the jet model was statistically indistinguishable from the measured value (b=0.17; Fig. 8A; Table 2). The paddle model greatly underestimated speed (a=–3.0), but overestimated the scaling factor of speed (b_{paddle}=0.33; Table 2). The hydrodynamic cost of transport decreased with

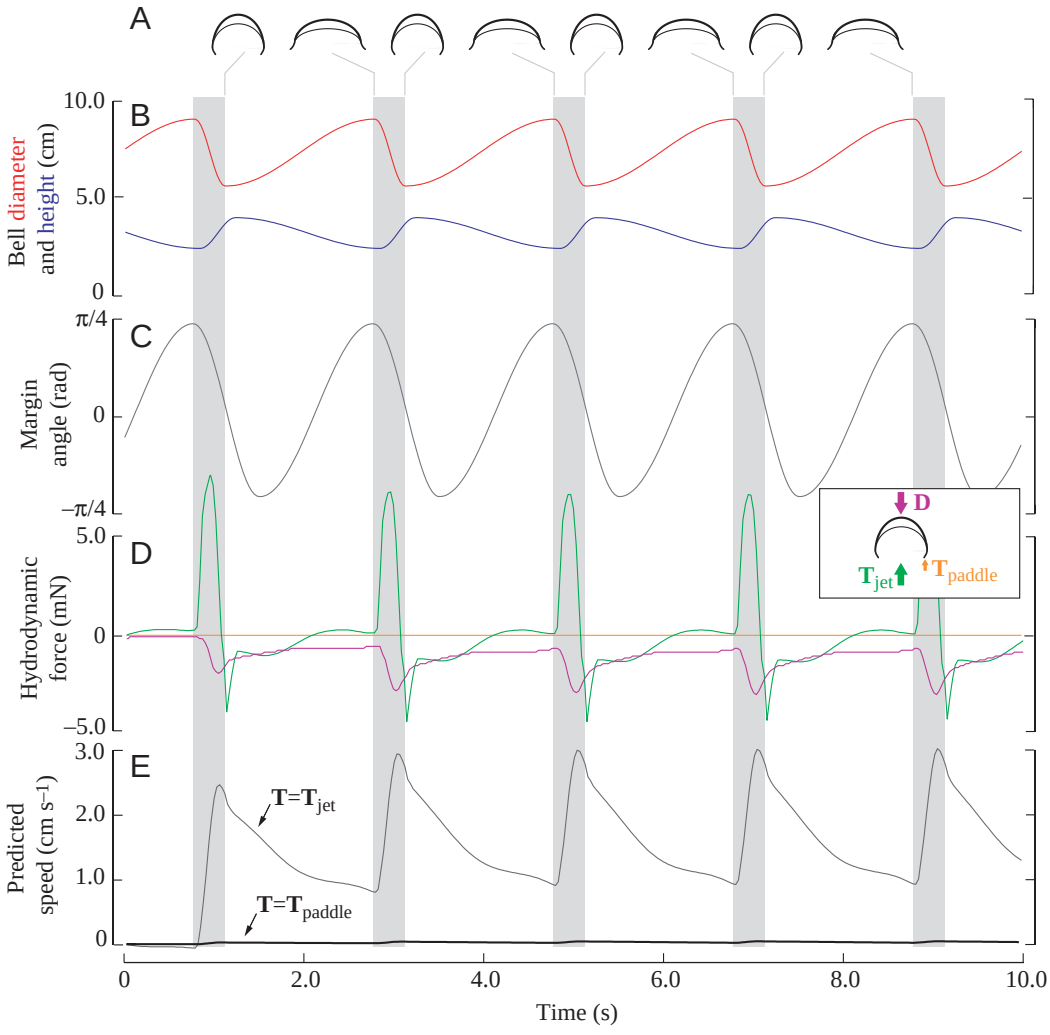

Fig. 3. A computational simulation of jellyfish swimming. (A) A schematic of the body illustrates its shape at the beginning and immediately following the pulse phase (gray bar) for each propulsive cycle. (B) The jet model calculated thrust production from changes in bell height (blue line) and diameter (red line) and (C) the paddle model calculated thrust from changes in margin angle. (D) The force predicted by jet thrust ($\mathbf{T}_{jet}$; green line), and drag (**D**; violet line) during a simulation of the jet model. The paddle thrust ($\mathbf{T}_{paddle}$; orange line) was generated in a separate simulation of the paddle model, and the drag generated during this simulation is not shown. (E) The changes in swimming speed predicted by paddle and jet models.

body mass (b=–0.62), but we formulated no null hypothesis for its scaling factor (Table 1; Fig. 8B) and its variation was not well described by a reduced major axis regression (r^2=0.05).

The effects of morphology and behavior on performance

We examined the effects of allometric and isometric growth on swimming performance with parameter maps for body mass and the height-to-diameter ratio (Fig. 9A,B). These parameter maps suggest that relatively large and prolate jellyfish swim faster than small and oblate jellyfish. If *Aurelia* maintained a prolate bell shape (as seen in the early medusa stage) over their entire ontogeny, then their mean swimming speed would be faster (2.7 cm s^{-1}) than the speed that we observed (1.9 cm s^{-1}) but they would swim with a higher hydrodynamic cost of transport (0.05 J kg^{-1} m^{-1}, compared with 0.04 J kg^{-1} m^{-1}). If they maintained an oblate bell shape (as seen in the late medusa stage), then jellyfish would swim slightly slower (1.6 cm s^{-1}) than what we observed but would have a lower hydrodynamic cost of transport (0.03 J kg^{-1} m^{-1}, Fig. 9A,B).

According to our parameter maps of pulse frequency and body mass, larger jellyfish with a relatively high pulse frequency move at faster speeds but with a dramatically greater hydrodynamic cost of transport compared with smaller jellyfish swimming with lower pulse frequencies (Fig. 9C,D). If *Aurelia* maintained a high pulse frequency (as seen in the early medusa stage) over ontogeny, they would swim faster (19.0 cm s^{-1}) but with a much greater hydrodynamic cost of transport (1.39 J kg^{-1} m^{-1}) than the swimming that results from the changes in pulse frequency that we observed (with a speed of 2.0 cm s^{-1} and a hydrodynamic cost of transport of 0.07 J kg^{-1} m^{-1}; Fig. 9C,D). Alternatively, if these jellyfish maintained a low pulse frequency (as seen in the late medusa stage) over ontogeny, then they would swim slower (0.01 cm s^{-1}) but with a much lower hydrodynamic cost of transport (0.01 J kg^{-1} m^{-1}).

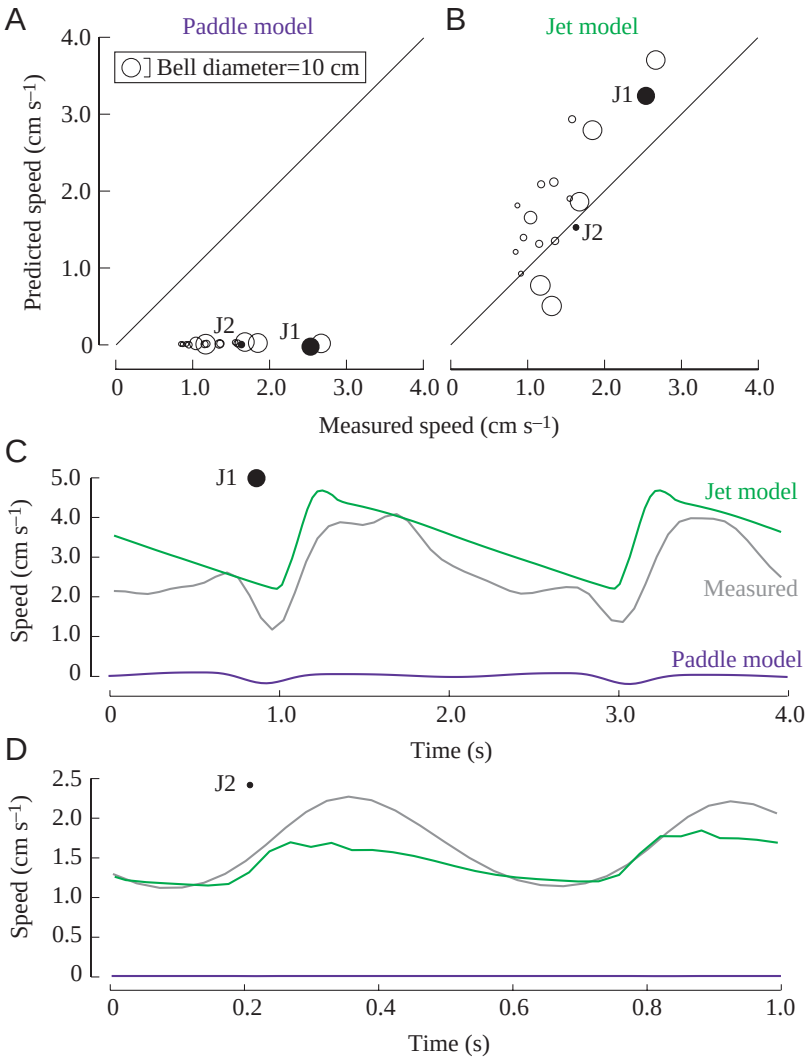

Fig. 4. An experimental test of paddle and jetting models for the hydrodynamics of swimming in *Aurelia aurita*. The relationship between the measured and predicted mean swimming is shown for the paddle model (A) and the jet model (B). The black line has a slope of 1, which represents a perfectly accurate prediction of measured speed (N=18). The diameter of points is proportional to the bell diameter of jellyfish (see legend for scale). Representative large (J1; bell diameter, 8.5 cm) and small (J2; bell diameter, 1.8 cm) jellyfish are highlighted in black. The speed predictions for each model are compared with measurements of speed for J1 (C) and J2 (D).

Discussion

The results of our experiments and mathematical simulations suggest that *Aurelia* swims by jet propulsion and that the relative magnitude of thrust, the acceleration reaction and drag changes over ontogeny (Figs 4, 7, 8). This change in hydrodynamics is the apparent result of an ontogenetic decrease in pulse frequency, which causes swimming speed and drag to scale below the factors predicted by kinematic similarity. By changing the shape of the bell to a more oblate morphology and by decreasing pulse frequency during growth, *Aurelia* avoids a relatively high cost of transport while swimming at a moderately high speed over their ontogeny (Fig. 9).

The hydrodynamics of jellyfish swimming

Prior to the present study, there was evidence suggesting that *Aurelia* does not generate thrust by jetting. Colin and Costello (2002) reported that Daniel's (1983) model of jetting underestimated maximum acceleration in hydromedusae with an oblate bell shape similar to that of *Aurelia*. Furthermore, *Aurelia* lacks the velum used by hydromedusae to force the

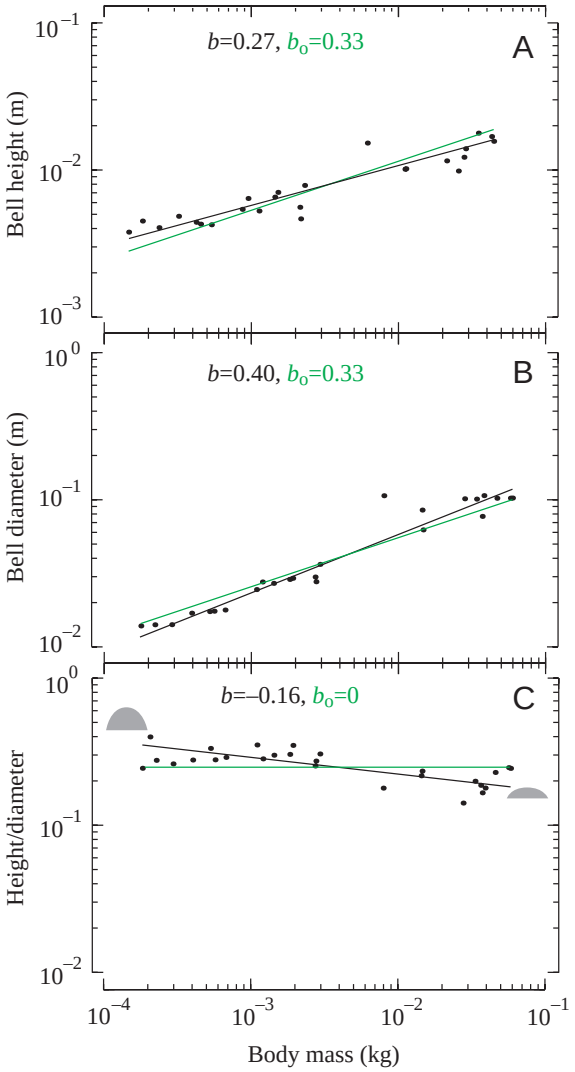

Fig. 5. The scaling of bell morphology with body mass. Linear regressions found by reduced major axis (black line; b) were significantly different (see Table 1 for statistics) from the null hypothesis (green line; b_o), which predicts geometric similarity in bell height (A), bell diameter (B) and the ratio of height to diameter (C). The gray silhouettes in C approximate the bell shape of small and large medusae.

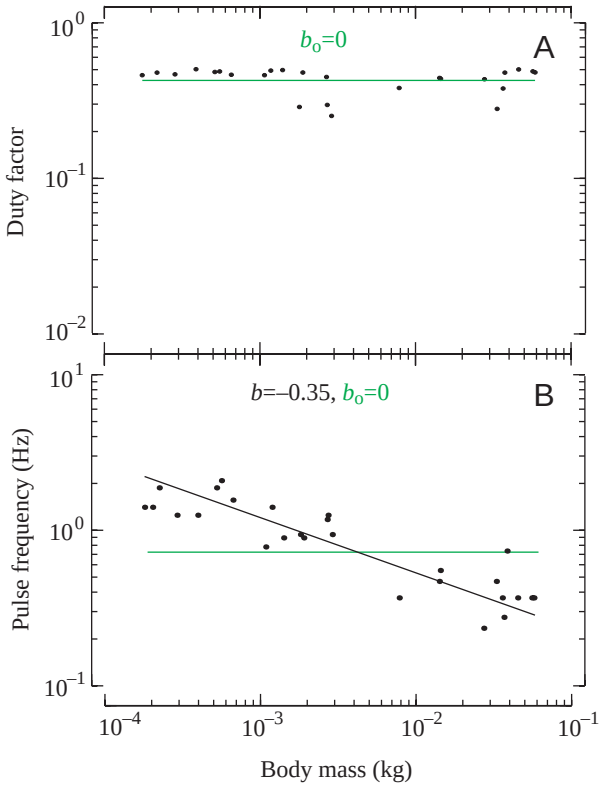

Fig. 6. The scaling of bell kinematics with body mass. The null hypothesis (green line; b_o), of kinematic similarity predicted constant values in duty factor and pulse frequency. (A) Duty factor was independent of body mass, as predicted by kinematic similarity. (B) The reduced major axis regression (black line; b) shows a decrease in pulse frequency with increasing body mass (see Table 1 for statistics).

water ejected from the bell cavity through a small hole. Lacking this membrane, it appeared unlikely that *Aurelia* transports water from the subumbrellar cavity as a cylindrical jet, which violates an assumption of the jet model (Daniel, 1983). Furthermore, flow visualization around the bodies of oblate jellyfish like *Aurelia* suggests that vortices are generated in close proximity to the bell during the pulse phase, which is an observation consistent with the hypothesis that the margin generates thrust (Colin and Costello, 2002; Costello and Colin, 1994). However, our results explicitly refute this hypothesis and lend support to the idea that thrust is generated by jetting (Figs 4, 8; Table 2).

Although not perfectly accurate, a jet model provides the best approximation of the hydrodynamics of swimming in oblate jellyfish like *Aurelia*. Unlike the paddle model, the jet model consistently predicted oscillations in speed with time that followed measured changes (Fig. 4C,D) and mean speed values that were within measured values by a factor of three (Fig. 4A,B). Furthermore, the jet model accurately predicted the scaling factor for swimming speed (Fig. 8A; Table 2). These successful predictions suggest that *Aurelia* generates thrust by jetting, as found in other jellyfish species (Colin and Costello, 2002; Daniel, 1983) and that the same hydrodynamic principles operate for all jellyfish species, regardless of bell morphology. However, the jet model did generally predict speeds that were greater than measured values (Figs 4B, 8A; Table 2), which is a result consistent with previously reported high estimates of maximum acceleration (Colin and Costello, 2002).

Discrepancies between performance measurements and jet model predictions suggest a need for refinement of our understanding of the hydrodynamics of oblate jellyfish. Daniel (1983) calculated the drag on the bell of prolate jellyfish using the drag coefficient for a sphere, but the shape of oblate species may be better approximated by a hemisphere, as in the present

Table 1. *Scaling with body mass*, m

Dependent variable, y	$y=am^b$ a	b	L_1	L_2	b_o	r^2
Morphometrics (N=25)						
d_{rest} (m)	–0.4	0.40*	0.36	0.44	0.33	0.94
h_{rest} (m)	–1.5	0.27*	0.23	0.31	0.33	0.87
h_{rest}/d_{rest}	–1.1	–0.16*	–0.19	–0.12	0	0.73
s_{rest}	–0.9	0.80*	0.72	0.89	0.66	0.94
l (m)	–1.0	0.43*	0.36	0.50	0.33	0.84
Kinematics (N=25)						
f (Hz)	–1.0	–0.35*	–0.41	–0.29	0	0.83
q	–0.63	–0.11*	–0.15	–0.06	0	0.02
d_{range} (m)	–0.80	0.42*	0.36	0.49	0.33	0.87
h_{range} (m)	–1.2	0.38	0.30	0.46	0.33	0.66
θ_{range} (rad)	0.98	0.29*	0.17	0.42	0	0.03
Hydrodynamics (N=25) (jet model)						
$\mathbf{D}_{max}$ (N)	–2.2	0.76*	0.68	1.1	1.33	0.74
$\mathbf{T}_{max}$ (N)	–0.22	1.3	1.1	1.5	1.33	0.84
$\mathbf{A}_{max}$ (N)	–0.50	1.3	1.1	1.5	1.33	0.87
Performance (N=18)						
$\mathbf{U}$ (m s^{-1})	–1.4	0.17*	0.10	0.24	0.33	0.53
T_{HCOT} (J kg^{-1} m^{-1})	–3.2	–0.60*	–0.92	–0.31	0.05	

a, scaling constant; b, scaling exponent (asterisks denote significant difference from b_o); L_1 lower limit of 95% confidence interval; L_2 upper limit of 95% confidence interval; b_o, null hypothesis; d_{rest}, resting bell diameter; h_{rest}, resting bell height; s_{rest}, projected area of the bell at rest; l, length of the bell margin; f, pulse frequency; q, duty factor; d_{range}, range of bell diameter; h_{range}, range of bell height; θ_{range}, range of margin angle; $\mathbf{D}_{max}$, maximum drag; $\mathbf{T}_{max}$ maximum thrust; $\mathbf{A}_{max}$ maximum acceleration reaction; $\mathbf{U}$, swimming speed; T_{HCOT}, hydrodynamic cost of transport.

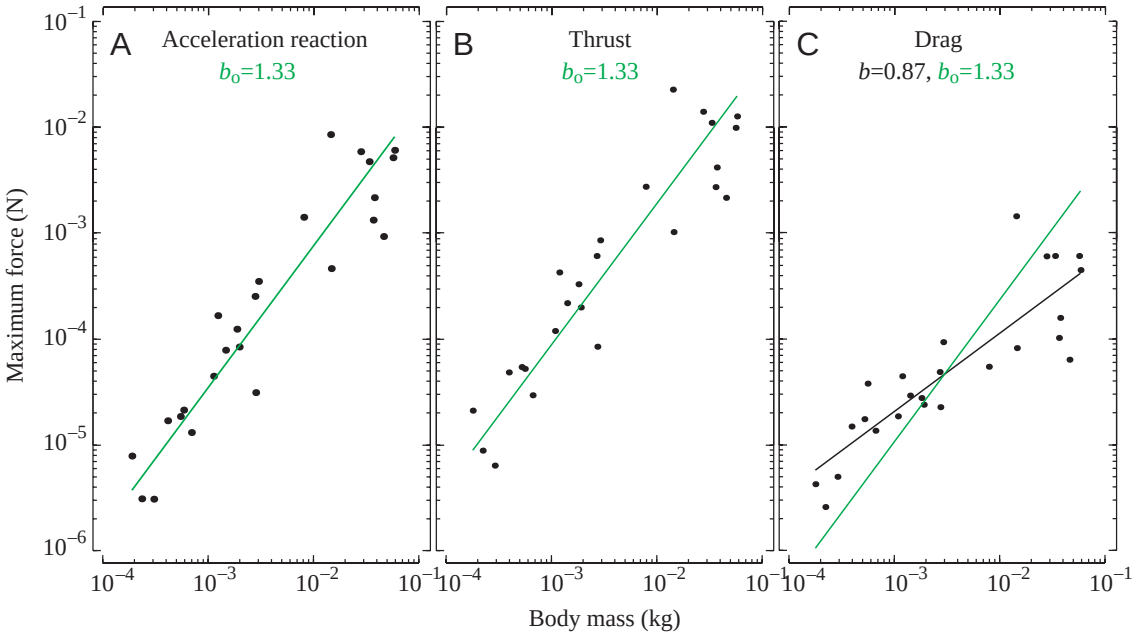

Fig. 7. The scaling of hydrodynamic forces predicted by the jet model. Maximum acceleration reaction (A) and thrust (B) scaled as predicted by kinematic similarity (green line; b_o), but drag (C) increased with a lower exponent (black line; b) than the null hypothesis (see Table 1 for statistics).

study. Furthermore, neither the present study nor Daniel (1983) considers the drag generated by the tentacles. Although we intuitively understand that the acceleration reaction should vary with the Reynolds number of a swimming animal (Daniel et al., 1992; Jordan, 1992; McHenry et al., 2003), we lack an equation that describes the relationship between the acceleration reaction coefficient (equation 6) and Reynolds number. Furthermore, flow visualization studies (Colin and

Costello, 2002; Costello and Colin, 1994) suggest that the jet of oblate jellyfish has a more complex wake pattern than the cylindrical column of water assumed in the present study. Future models should become more predictive as they incorporate more of this hydrodynamic complexity.

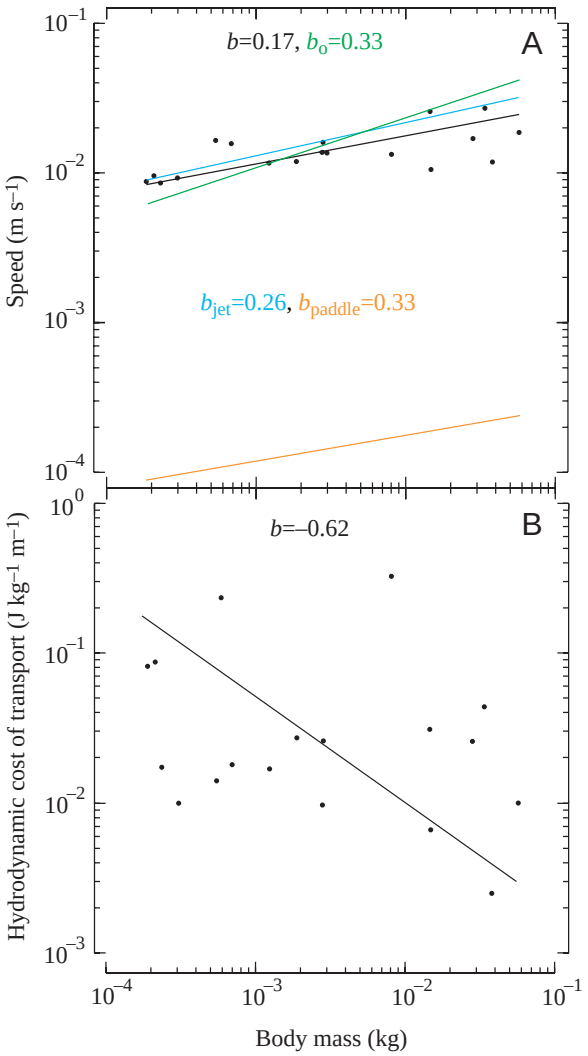

Fig. 8. The scaling of swimming performance. (A) The null hypothesis (green line; b_o) was significantly different from the reduced major axis regression for measurements of swimming speed (black line; b). The measured scaling factor was not significantly different from predictions for the jet model (blue line; b_{jet}), but was significantly different for the paddle model (orange line; b_{paddle}; see Table 2 for statistics). (B) There was no null hypothesis predicted for the hydrodynamic cost of transport (see Table 1 for statistics).

The scaling of swimming performance

The hydrodynamic changes over the growth of *Aurelia* are reflected in the different scaling relationships of the three fluid forces considered (Fig. 7). Although maximum values of thrust and the acceleration reaction scale at rates consistent with kinematic similarity, swimming speed scales at a rate below that predicted by kinematic similarity (Fig. 8A). Therefore, larger jellyfish swim disproportionately slower than smaller jellyfish, and drag consequently scales at a lower factor than predicted by kinematic similarity (Fig. 7C). This low scaling factor for drag occurs despite the fact that the projected area of the bell scales with a higher factor than predicted by geometric similarity (Table 1). According to our model, the scaling of speed is influenced by the ontogenetic decrease in pulse frequency (Fig. 6B). When pulse frequency was held constant in our simulations, speed increased rapidly with increasing body mass (Fig. 9C). This suggests that it is the rate, not the magnitude, of force production that caused speed and drag to scale by a factor below that predicted by kinematic similarity.

Although fish swim by lateral undulation instead of jetting, their swimming speed is also strongly dependent on the frequency of the propulsive cycle. Speed increases linearly with tail beat frequency in a diversity of species (Jayne and Lauder, 1995; Long et al., 1994, 1996; Webb, 1986). However, when fish of different size within a species are made to swim at the same frequency, they move at the same length-specific speed (Bainbridge, 1958). Such kinematic similarity could exist in jellyfish if they maintained the same pulse frequency over a range of body size.

Our results suggest that ontogenetic changes in the body shape and pulse frequency of *Aurelia* influence a tradeoff between swimming speed and the cost of transport. By changing from a prolate to oblate bell shape, *Aurelia* grows from a shape of relative high speed and high cost to one of low speed and low cost (Fig. 9A,B). However, the difference in mean performance between allometric and isometric growth is subtle, when compared to the effects of pulse frequency. By reducing pulse frequency over ontogeny, *Aurelia* avoids the dramatically high cost of transport predicted for large jellyfish that maintain a high pulse frequency (Fig. 9D), but this decrease in frequency comes at a cost to speed (Fig. 9C).

Table 2. *Scaling of swimming speed predicted by mathematical models*

		Jet model			Paddle model		
$u=am^b$	Measured	Predicted	L_1	L_2	Predicted	L_1	L_2
b	0.17	0.26	0.13	0.39	0.33*	0.19	0.48
a	–1.4	–1.1*	–1.2	–1.0	–3.0*	–3.1	–2.9

u, swimming speed; m, body mass; a, scaling constant; b, scaling exponent (asterisks denote significant difference from measurement); L_1 lower limit of 95% confidence interval; L_2 upper limit of 95% confidence interval; N=18.

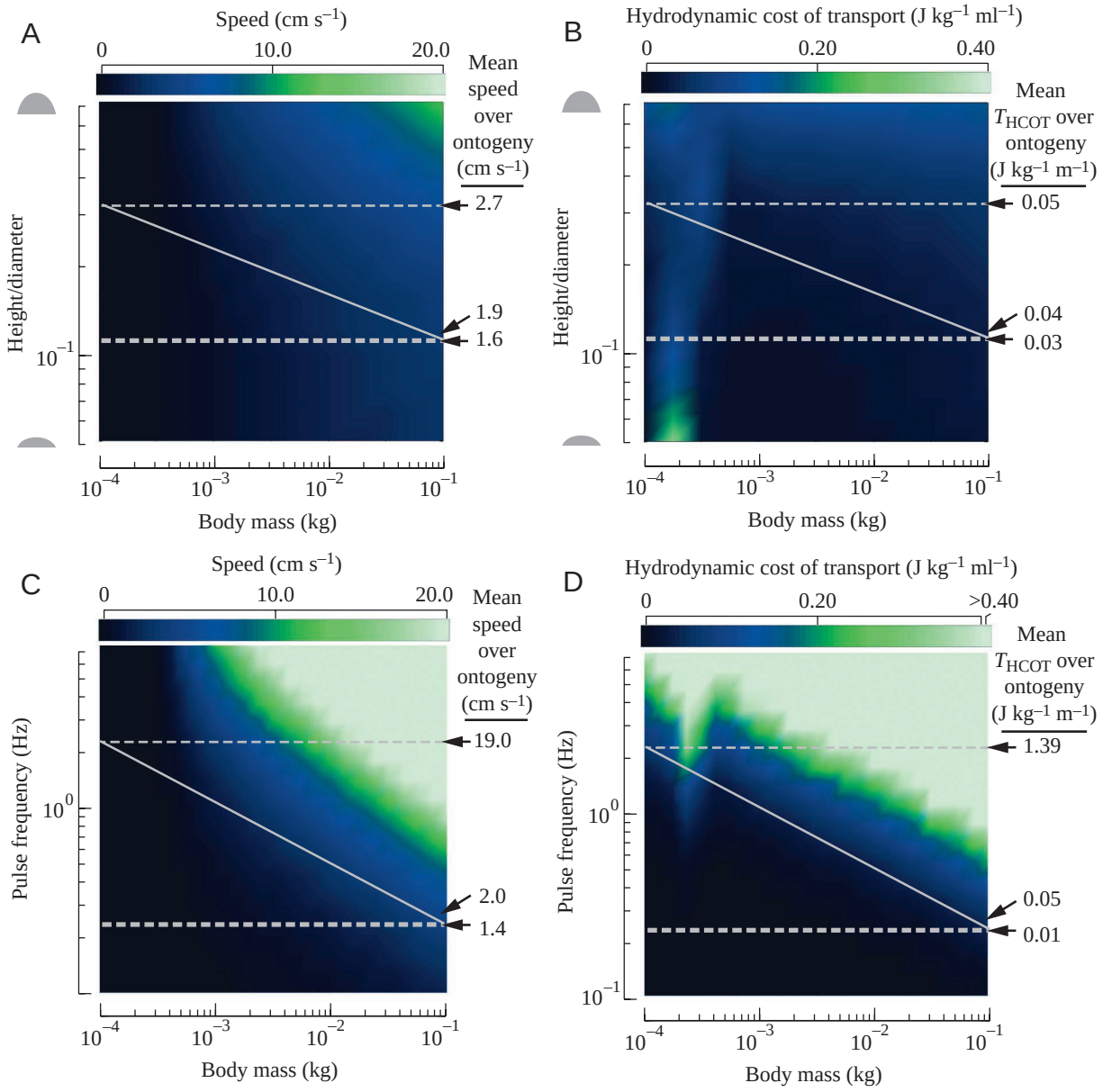

Fig. 9. Parameter maps show how the scaling of the height-to-diameter ratio and pulse frequency with body mass is predicted to affect swimming speed and the hydrodynamic cost of transport. Gray lines follow patterns of ontogenetic change, and the performance values to the right of these lines are the mean performance predicted over ontogeny. (A,B) Gray silhouettes show the shape of the bell at high (prolate) and low (oblate) height to diameter values. The thin, broken, horizontal line shows isometric scaling where the jellyfish maintain a prolate morphology at all sizes, the solid line follows the allometric scaling that we measured (Fig. 5), and the thick, broken, horizontal line shows the isometric scaling where jellyfish maintain an oblate morphology at all sizes. (C,D) The thin, broken, horizontal line follows a constant high value of pulse frequency at all body sizes, the solid line tracks the change in frequency that we measured (Fig. 6), and the thick, broken, horizontal line maintains a constant low value for pulse frequency at all body sizes. (D) Notice that we have coded values for the hydrodynamic cost of transport (T_{HCOT}) exceeding 0.40 J kg^{-1} m^{-2} as light green in order to maintain a scale that results in visible typography for the rest of this parameter map.

Our results support the hypothesis that medusae change their behavior and morphology to maintain a moderate speed while avoiding a high cost of transport. However, it is difficult to weigh the relative importance of speed and the cost of transport to the ecology and evolution of *Aurelia* without an understanding of how these aspects of performance influence fitness (Koehl, 1996). Furthermore, ontogenetic changes in behavior and morphology may influence other aspects of organismal performance that have a greater effect on fitness than does locomotion. For this reason, it would be interesting to explore how these ontogenetic changes affect prey capture and mass transport.

Performance and growth

The effect that the shape of an organism has on its mechanical performance is likely to change during growth because biomechanical forces are typically scale dependent. Therefore, changes in shape may reflect a shift in the mechanical demands of larger structures. Alternatively, morphology may change in order to meet other physiological demands or because of developmental constraints. In the interest of understanding why organisms change or preserve shape during growth, it is useful to compare the ontogenetic changes in morphology that organisms exhibit to alternate patterns of growth. For example, Gaylord and Denny (1997) used a mathematical model to examine how different patterns of growth in seaweeds (*Eisenia arborea* and *Pterygophora californica*) affected their susceptibility to breakage in intertidal habitats. They found that the allometric growth exhibited by these organisms results in lower material stress than if the seaweeds maintained their juvenile shape over their life history. Similarly, we found that jellyfish have a lower energetic cost of swimming by changing their bell shape over ontogeny than if they maintained the prolate shape of juveniles (Fig. 9B). In aquatic animals, ontogenetic change in performance may be strongly influenced by changes in behavior. For example, we found that changes in pulse frequency have an even stronger effect on performance than the changes in bell shape (Fig. 9).

It would be difficult to explore alternate patterns of growth or to tease apart the individual effects of morphological and kinematic parameters without the use of a mathematical model. In order for such models to accurately predict performance, they require accurate parameter values that are provided by measurements. Therefore, the integration of theoretical and experimental approaches should greatly facilitate our understanding of how ontogenetic changes in morphology or behavior affect organismal performance.

List of symbols

a	scaling constant
$\mathbf{A}$	acceleration reaction force
b	scaling exponent
b_o	null hypothesis
c_{bell}	drag coefficient for the bell
c_{margin}	drag coefficient for the bell margin
d	bell diameter
d_{range}	range of bell diameter
d_{rest}	resting bell diameter
$\mathbf{D}$	drag
e	slope of major axis regression
f	pulse frequency
$\mathbf{F}$	force to change body inertia
h	bell height
h_{cav}	height of subumbrellar cavity
h_{range}	range of bell height
h_{rest}	resting bell height
i	index of measurements
k	sawtooth function
l	length of the bell margin
L_1	lower limit of 95% confidence interval
L_2	upper limit of 95% confidence interval
m	body mass
n	number of measurements
q	duty factor
s_{bell}	projected area of the bell
s_{margin}	area of the bell margin
t	time
$\mathbf{T}$	thrust
T_{HCOT}	hydrodynamic cost of transport
$\mathbf{T}_{jet}$	thrust generated by a jet
$\mathbf{T}_{paddle}$	thrust generated by a paddle
u	swimming speed
$\mathbf{U}$	body velocity
v	volume of the subumbrellar cavity
w	speed of the bell margin
$\mathbf{W}$	velocity of the bell margin
x	net distance
y	dependent variable
α	added mass coefficient
θ	margin angle
θ_{range}	range of margin angle
ρ_{tissue}	density of tissue
ρ_{water}	density of seawater

We thank M. Koehl and T. Daniel for their guidance and advice, and A. Summers, W. Korff, J. Nauen and J. Strother for their suggestions. This work was supported with an NSF predoctoral fellowship and grants-in-aid of research from the American Society of Biomechanics, Sigma Xi, the Department of Integrative Biology (U.C. Berkeley) and the Society for Integrative and Comparative Biology to M.J.M. Additional support came from grants from the National Science foundation (# OCE-9907120) and the Office of Naval Research (AASERT # N00014-97-1-0726) to M. Koehl.

References

Bainbridge, R. (1958). The speed of swimming fish as related to size and to the frequency and amplitude of the tail beat. *J. Exp. Biol.* **35**, 109-133.

Batchelor, G. K. (1967). *An Introduction to Fluid Dynamics*. New York: Cambridge University Press.

Batty, R. (1984). Development of swimming movements and musculature of larval herring (*Clupea harengus*). *J. Exp. Biol.* **110**, 217-229.

Buecher, E. and Gibbons, M. J. (1999). Temporal persistence in the vertical structure of the assemblage of planktonic medusae in the NW Mediterranean Sea. *Mar. Ecol. Prog. Ser.* **189**, 105-115.

Colin, S. P. and Costello, J. H. (2002). Morphology, swimming performance and propulsive mode of six co-occurring hydromedusae. *J. Exp. Biol.* **205**, 427-437.

Costello, J. H. and Colin, S. P. (1994). Morphology, fluid motion and predation by the scyphomedusa *Aurelia aurita*. *Mar. Biol.* **121**, 327-334.

Dadswell, M. J. and Weihs, D. (1990). Size-related hydrodynamic characteristics of the giant scallop, *Placopecten magellanicus* (Bivalvia: Pectinidae). *Can. J. Zool.* **68**, 778-785.

Daniel, T., Jordan, C. and Grunbaum, D. (1992). Hydromechanics of swimming. In *Advances in Comparative and Environmental*

Physiology, vol. 11 (ed. R. McN. Alexander), pp. 17-49. London: Springer-Verlag.
Daniel, T. L. (1983). Mechanics and energetics of medusan jet propulsion. *Can. J. Zool.* **61**, 1406-1420.
Daniel, T. L. (1985). Cost of locomotion: Unsteady medusan swimming. *J. Exp. Biol.* **119**, 149-164.
Fuiman, L. A. (1993). Development of predator evasion in Atlantic herring, *Clupea harengus* L. *Anim. Behav.* **45**, 1101-1116.
Fuiman, L. A. and Batty, R. S. (1997). What a drag it is getting cold: partitioning the physical and physiological effects of temperature on fish swimming. *J. Exp. Biol.* **200**, 1745-1755.
Fuiman, L. A. and Webb, P. W. (1988). Ontogeny of routine swimming activity and performance in zebra danios (Teleostei: Cyprinidae). *Anim. Behav.* **36**, 250-261.
Gaylord, B. and Denny, M. W. (1997). Flow and flexibility. I. Effects of size, shape and stiffness in determining wave forces on the stipitate kelps *Eisenia arborea* and *Pterygophora californica*. *J. Exp. Biol.* **200**, 3141-3164.
Gladfelter, W. G. (1973). A comparative analysis of the locomotory system of medusoid Cnidaria. *Helgol. Wiss. Meeresunters* **25**, 228-272.
Hale, M. (1999). Locomotor mechanics during early life history: effects of size and ontogeny on fast-start performance of salmonid fishes. *J. Exp. Biol.* **202**, 1465-1479.
Hernandez, L. P. (2000). Intraspecific scaling of feeding mechanics in an ontogenetic series of zebrafish, *Danio rerio*. *J. Exp. Biol.* **203**, 3033-3043.
Hoerner, S. F. (1965). *Fluid-Dynamic Drag*. Brick Town, NJ: Hoerner Fluid Dynamics.
Hunter, J. R. (1972). Swimming and feeding behavior of larval anchovy *Engraulis mordax*. *Fish. Bull.* **70**, 821-838.
Hunter, J. R. and Kimbrell, C. A. (1980). Early history of pacific mackerel, *Scomber japonicus*. *Fish. Bull.* **78**, 89-101.
Huxley, J. S. (1932). *Problems of Relative Growth*. New York: Dial Press.
Jayne, B. C. and Lauder, G. V. (1995). Speed effects on midline kinematics during steady undulatory swimming of largemouth bass, *Micropterus salmoides*. *J. Exp. Biol.* **198**, 585-602.
Johnson, D. R., Perry, H. M. and Burke, W. D. (2001). Developing jellyfish strategy hypotheses using circulation models. *Hydrobiology* **451**, 213-221.
Jordan, C. E. (1992). A model of rapid-start swimming at intermediate Reynolds number: undulatory locomotion in the chaetognath *Sagitta elegans*. *J. Exp. Biol.* **163**, 119-137.
Koehl, M. A. R. (1996). When does morphology matter? *Annu. Rev. Ecol. Syst.* **27**, 501-542.
Lighthill, J. (1975). *Mathematical Biofluidynamics*. Philadelphia: Society for Industrial and Applied Mathematics.
Long, J. H., Hale, M. E., McHenry, M. J. and Westneat, M. W. (1996). Functions of fish skin: flexural stiffness and steady swimming of longnose gar *Lepisosteus osseus*. *J. Exp. Biol.* **199**, 2139-2151.
Long, J. H., McHenry, M. J. and Boetticher, N. C. (1994). Undulatory swimming: how traveling waves are produced and modulated in sunfish (*Lepomis gibbosus*). *J. Exp. Biol.* **192**, 129-145.
McHenry, M. J., Azizi, E. and Strother, J. A. (2003). The hydrodynamics of undulatory swimming at intermediate Reynolds numbers in ascidian larvae (*Botrylloides* sp.). *J. Exp. Biol.* **206**, 327-343.
McMahon, T. A. (1984). *Muscles, Reflexes, and Locomotion*. Princeton, NJ: Princeton University Press.
Meinkoth, N. A. (1995). *National Audubon Society Field Guide to North American Seashore Creatures*. New York: Alfred A. Knopf, Inc.
Mills, C. E. (1981). Diversity of swimming behaviors in hydromedusae as related to feeding and utilization of space. *Mar. Biol.* **64**, 185-189.
Muller, U. K., Stamhuis, E. J. and Videler, J. J. (2000). Hydrodynamics of unsteady fish swimming and the effects of body size: comparing the flow fields of fish larvae and adults. *J. Exp. Biol.* **203**, 193-206.
Mutlu, E. (2001). Distribution and abundance of moon jellyfish (*Aurelia aurita*) and its zooplankton food in the Black Sea. *Mar. Biol.* **138**, 329-339.
Nauen, J. and Shadwick, R. (2001). The dynamics and scaling of force production during the tail-flip escape response of the California spiny lobster *Panulirus interruptus*. *J. Exp. Biol.* **204**, 1817-1830.
Nicholas, K. R. and Frid, C. L. J. (1999). Occurrence of hydromedusae in the plankton off Northumberland (western central North Sea) and the role of planktonic predators. *J. Mar. Biol. Assoc. UK* **79**, 979-992.
Osse, J. W. M. and van den Boogaart, J. G. M. (2000). Body size and swimming types in carp larvae: effects of being small. *Neth. J. Zool.* **50**, 233-244.
Quillin, K. J. (1999). Kinematic scaling of locomotion by hydrostatic animals: ontogeny of peristaltic crawling by the earthworm *Lumbricus terrestris*. *J. Exp. Biol.* **202**, 661-674.
Quillin, K. J. (2000). Ontogenetic scaling of burrowing forces in the earthworm *Lumbricus terrestris*. *J. Exp. Biol.* **203**, 2757-2770.
Rayner, J. M. V. (1985). Linear relations in biomechanics – the statistics of scaling functions. *J. Zool.* **206**, 415-439.
Rome, L. (1992). Scaling of muscle fibers and locomotion. *J. Exp. Biol.* **168**, 243-252.
Schmidt-Nielsen, K. (1984). *Scaling: Why is Animal Size so Important*? Cambridge: Cambridge University Press.
Shampine, L. F. and Gordon, M. K. (1975). *Computer Solution of Ordinary Differential Equations: The Initial Value Problem*. San Francisco: W. H. Freeman.
Sokal, R. R. and Rohlf, F. J. (1995). *Biometry*. New York: W. H. Freeman & Co.
Vlymen, W. J. (1974). Swimming energetics of the larval anchovy *Engraulis mardax*. *Fish. Bull.* **72**, 885-899.
Vogel, S. (1981). *Life in Moving Fluids*. Princeton: Princeton University Press.
Webb, P. W. (1986). Kinematics of lake sturgeon, *Acipenser fulvescens*, at cruising speeds. *Can. J. Zool.* **64**, 2137-2141.
Webb, P. W. and Weihs, D. (1986). Functional locomotor morphology of early life-history stages of fishes. *Trans. Am. Fish. Soc.* **115**, 115-127.
Williams, T. A. (1994). A model of rowing propulsion and the ontogeny of locomotion in *Artemia* larvae. *Biol. Bull.* **187**, 164-173.
Wu, T. Y. (1977). Introduction to the scaling of aquatic animal locomotion. In *Scale Effects in Animal Locomotion* (ed. T. J. Peldley), pp. 203-232. London: Academic Press.